AAS 15-053

Performance Optimization Study for Touchless Electrostatic Spacecraft De-spin Operations

Daan Stevenson
Hanspeter Schaub

University of Colorado Boulder

38th ANNUAL AAS GUIDANCE AND CONTROL CONFERENCE

January 30 - February 4, 2015
Breckenridge, Colorado

Sponsored by
Rocky Mountain Section

AAS Publications Office, P.O. Box 28130 - San Diego, California 92198

AAS 15-053

PERFORMANCE OPTIMIZATION STUDY FOR TOUCHLESS ELECTROSTATIC SPACECRAFT DE-SPIN OPERATIONS

Daan Stevenson* **and Hanspeter Schaub†**

An electrostatic de-spin concept has been proposed for remotely removing excess rotation rates from uncontrolled satellites in the GEO orbit regime. While the 1D-dynamics and control of this system have already been analyzed extensively, a study is herein conducted to determine how to optimize the performance of the system for future mission design. First, two different methods for simulating the baseline Coulomb de-spin system are presented. Then, the sensitivity of de-spin time, required thrust profiles, and system displacement to variations in spacecraft sizes, shapes, and separation distance is considered. The findings show that increasing the size of the servicing craft results in diminishing returns in performance, and that the optimal aspect ratio of the targeted debris satellite is quite low, assuming constant density. Furthermore, various position and attitude control schemes for the servicing craft are studied to see if the de-spin time can be reduced. Performance is improved considerably by varying the relative position to maintain a minimum surface to surface distance or by circumnavigating the debris to operate with maximum control torques, but both approaches significantly increase the required thrust magnitudes and fuel expenditure. Another promising approach is one where the servicing craft adjusts its attitude to position multiple voltage controlled features so that they impart optimal arresting torques on the spinning debris object.

INTRODUCTION

In order to ameliorate the ever increasing space situational awareness risks at Geosynchronous (GEO) orbits, spacecraft rendezvous is desirable for servicing or repositioning operations.[1] When large GEO spacecraft loose station keeping control, they can acquire sizable rotational momenta that imperil proximity operations and docking. Pose algorithms and attitude matching maneuvers for rendezvous are generally restricted to rotation rates below 1 deg/s,[2] thus limiting the viable targets for a physical docking strategy. Because non-cooperative spacecraft at GEO often exhibit large moments of inertia and rotational kinetic energy, a touchless method for reducing the rotation rate prior to rendezvous is desired.

Recent studies have identified the feasibility of touchless de-spin operations using electrostatic interactions with a nearby charge controlled spacecraft.[3,4] This technology concept is outlined in Figure 1, where the servicing spacecraft uses ion and electron emitters to impose equal or opposite polarity electrostatic potentials on the two craft. Due to its non-spherical geometry and close proximity with the charge control craft, the tumbling satellite experiences significant Coulomb torques. By implementing appropriate charge control algorithms,[5,6] these torques can be used to de-spin the

*Graduate Student, Aerospace Engineering Sciences, University of Colorado Boulder.
†Professor, Aerospace Engineering Sciences, University of Colorado Boulder.

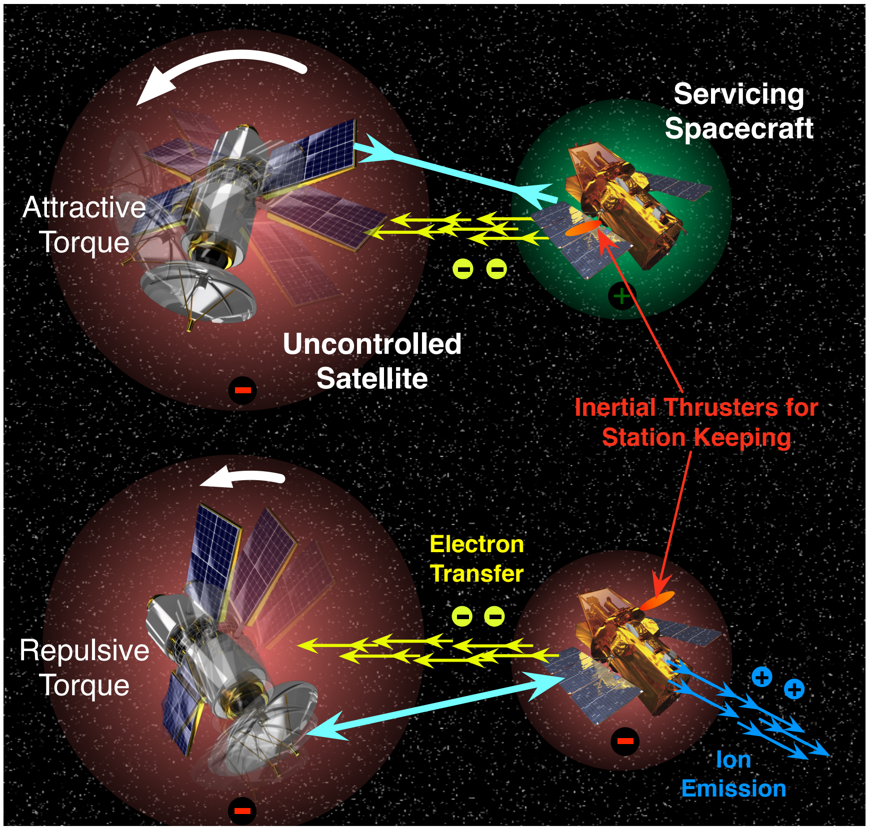

Figure 1. Depiction of remote electrostatic spacecraft de-spin concept

uncontrolled satellite, thus enabling further rendezvous and docking procedures. Because the electrostatic interaction also results in attractive or repulsive forces between the craft, inertial thrusters are required on the servicing spacecraft to maintain the desired relative motion in the formation.

In order to develop robust charge control algorithms and create 6-DOF simulations of the Coulomb de-spin system, faster than real time determination of the electrostatic interaction between the spacecraft is necessary. Finite element approaches are too computationally expensive to achieve this, while simplified point and sphere models fail to capture torques and off-axis forces. The Multi-Sphere Method (MSM)[7,8] can model a charged spacecraft geometry using a collection of conducting spheres. Computation is limited to inverting an $n \times n$ matrix (where n is the number of spheres in the system) to obtain the charge on each sphere, followed by a summation of Coulomb's law for each sphere to determine the resulting forces and torques. The spheres can be populated throughout a given volume, or more densely spaced along the surface of a geometry, which results in a trade off between accuracy and computational costs.

Previous studies have utilized this electrostatic model with varying amounts of spheres to analyze the de-spin dynamics and control requirements of a simplified cylinder-sphere system.[7,5,3] The concept has also been validated experimentally using a custom high voltage terrestrial testbed.[9,4] While the dimensions vary between investigations, the system configuration tends to remain fixed within any given study. To optimize the design of future mission scenarios, knowledge of the impact of various system parameters on de-spin performance is necessary. The following section presents the baseline simulations that are used for the ensuing sensitivity analysis. First, variations in separation distance as well as size and shape scaling of both spacecraft are studied to determine what effect they have on the system's de-spin time, displacement, and required stationkeeping maneuvers. In the last section, various relative position and orientation control schemes are considered to determine whether the location, or in the case of a nonspherical control craft its attitude, may be adjusted to reduce the de-spin time.

BASELINE SIMULATIONS

The simplified cylinder-sphere system in Figure 2 has generally been used to study the remote spacecraft attitude control problem.[5] Angular motion of the cylinder, which might represent an upper stage rocket body such as the Centaur, is limited to 1-D rotation about its major axis of inertia, while the nearby spherical control craft enforces the desired electrostatic potential on the two bodies. It is assumed here that negative voltage levels up to $\phi_2 = -30$ kV are achievable on the debris cylinder, while both polarity voltage levels up to $\phi_1 = \pm 30$ kV are achievable on the circular control craft. Other bodies of work study the requirements of the charge transfer devices necessary to achieve this remote control.[10,11] The electrostatic interaction between the objects results in equal and opposite Coulomb forces $F_1 = -F_2$ on the two bodies and a control torque L_2 on the rotating cylinder.

The recently developed Multi Sphere Model (MSM)[7] is employed to capture the 3D electrostatic effects with a set of conductive spheres distributed throughout the geometry of the spacecraft. The MSM relies on the mutual capacitance relationship between charged spheres. Assuming a known potential is prescribed on each of the n spheres in the system, a linear system of equations can be constructed to relate the charges on the spheres to their potentials. Once this system is solved, Coulomb's law is used to determine the force on each sphere, which sum to yield the total force and torque acting on each spacecraft.

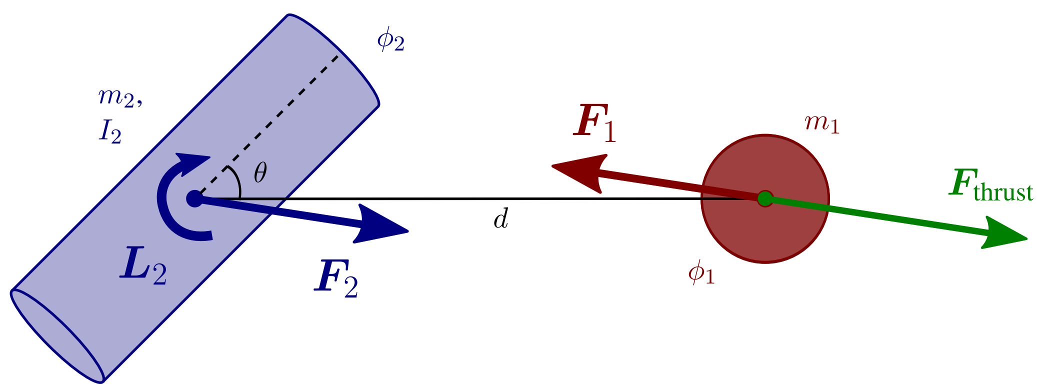

Figure 2. Free body diagram for cylinder-sphere system

In order to analyze the performance sensitivity of the remote de-spin concept, a baseline system must be defined. A representative debris cylinder with a length of 3 m and diameter of 1 m is selected, with a control craft of 1m diameter. Assuming an average density of 100 kg/m^3, this results in a 235.6 kg debris object with a $1,038.43$ kg-m^2 transverse moment of inertia and a 52.4 kg control craft. A $d = 7$ m separation is considered, which represents a surface to surface separation of 10 craft radii when the cylinder is oriented parallel and at closest approach. It is assumed that the debris object has an initial counter-clockwise rotation rate of $\omega = \dot{\theta} = 2$ rpm $= 12$ deg/s. The charge control algorithm is simplified so that $\phi_1 = 30$ kV and $\phi_2 = -30$ kV when $0^\circ < \theta < 90^\circ$, while $\phi_1 = \phi_2 = -30$ kV when $90° < \theta < 180°$, ensuring constantly arresting torques. A thrusting force

$$\boldsymbol{F}_{\text{thrust}} = -\boldsymbol{F}_1\left(1 + \frac{m_1}{m_2}\right) \tag{1}$$

is applied to the control craft in order to maintain a constant separation distance between the objects in space, resulting in a system acceleration

$$\boldsymbol{a}_{\text{sys}} = \frac{\boldsymbol{F}_2}{m_2} \tag{2}$$

When comparing the effect of various system parameters on de-spin performance, a simplified simulation is used where actuation averages are considered throughout one rotation of the debris cylinder. Since only a single rotation is considered, a higher fidelity surface Multi-Sphere Model (SMSM)[8] as shown in Figure 3 can be implemented, where 50 conducting spheres are evenly distributed along the surface of the debris cylinder and 13 spheres are used to model the control craft. As the cylinder completes one rotation, the electrostatic forces and torques are tracked. The average torque $L_{2,\text{ave}}$, which is independent of rotation rate, is used to calculate the de-spin time

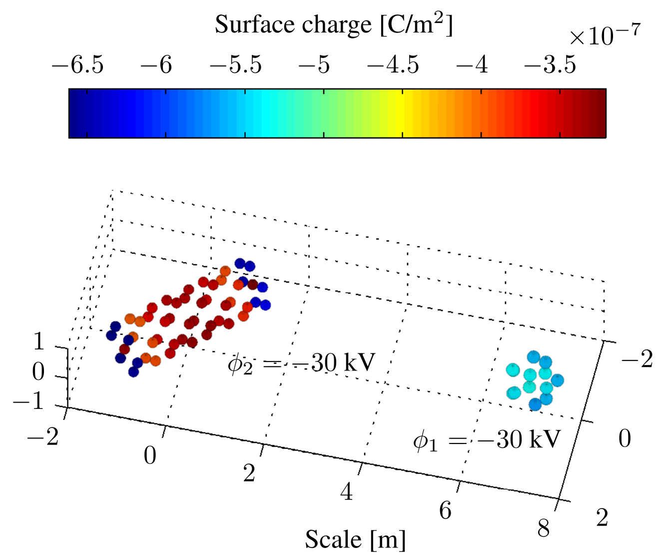

Figure 3. SMSM for cylinder-sphere system

$$\Delta t = \frac{I_2 \Delta\omega}{L_{2,\text{ave}}} \tag{3}$$

Given the de-spin time, the total system displacement in deep space can be calculated

$$\Delta \boldsymbol{X} = \frac{1}{2}\boldsymbol{a}_{\text{sys,ave}}\Delta t^2 = \frac{1}{2}\left(\frac{\boldsymbol{F}_{2,\text{ave}}}{m_2}\right)\Delta t^2 \tag{4}$$

The results for the single rotation simulation can be seen in the top line of Table 1. Coulomb forces and torques are quite low, but the control craft is still able to remove the 12 deg/s of rotation in just over 3 days, which is very promising for this type of operation. During that time, the entire system is displaced several dozens of kilometers, which could be used to raise the orbit of a GEO debris satellite and benefit the eventual goal of placing the object into a disposal orbit. If the system displacement is not desired, the control craft could reposition itself to opposite sides of the rotating debris in order to achieve a net zero system displacement. Because of the induced electrostatic effects and complex capacitance relationship between charge and voltage, there is a noticeable difference in performance between the pulling and pushing configurations in different quadrants. Namely, 62.4% of the arresting torque comes from the quadrants in which the debris object and control craft have opposite polarity (pulling configuration), while only 37.6% of the effort

Table 1. Baseline de-spin results

	$F_{2,\text{ave}}$ [mN]	$L_{2,\text{ave}}$ [mNm]	Δt [hrs]	ΔX [km]
Single Rotation Average	0.219	0.150	74.43	33.37
Time Dependent Simulation	0.225	0.150	74.32	34.35

comes from the equal polarity (pushing) configuration. The resulting difference in forces accounts for the net system displacement.

For the relative position and motion control schemes analyzed later on in the manuscript, a more detailed simulation is required. The de-spin operation is modeled from start to finish using an RK-45 integration, rather than extrapolating performance from a single cylinder rotation. The debris' attitude is restricted to rotation about its minor geometrical axis as before, but both objects have full translational freedom. The thrust control in Eq. (1) is implemented along with a proportional derivative feedback on the desired relative position. The same baseline parameters as above are used for the initial conditions of this simulation as well as the simple quadrant dependent voltage control. In order to limit the computation time for this simulation, the three sphere MSM outlined in Reference 7 is used to model the electrostatic interaction in the system. As is evident from Table 1, the resulting Coulomb torques and the total de-spin time agree to within a fraction of a percent with the single rotation simulation. The Coulomb force results agree to within 2.7% while system displacements deviate by about a kilometer, which results from extra errors in the discrete position feedback control algorithm. An average thrust magnitude of 1.30 mN is required to maintain the relative position in the system. If an ion thruster with $I_{SP} = 3000$ s is utilized, this results in 11.9 g of propellant expelled over the duration of the de-spin operation.

SYSTEM PARAMETER OPTIMIZATION

Separation Distance

It is important to understand the effect of separation distance on de-spin performance to determine what collision risks are warranted when conducting a remote electrostatic de-spin mission. Logically, the average force and torque experienced by the debris object decrease when the servicing craft is situated farther away. When varying the separation distance in the single rotation simulation discussed above, it is possible to fit the following functions with high correlation to the averaged Coulomb force and torque acting on the debris cylinder:

$$F_{2,\text{ave}} \approx 0.2136\, d^{-3.573}, \quad R^2 = 0.9974 \tag{5}$$

$$L_{2,\text{ave}} \approx 0.1076\, d^{-3.407}, \quad R^2 = 0.9985 \tag{6}$$

Since the time to remove a given rotation rate varies inversely with the average Coulomb torque, and combining Eqs. (3) and (4) yields

$$\Delta X = \frac{1}{2}\left(\frac{{I_2}^2 \Delta\omega^2}{m_2}\right)\left(\frac{F_{2,\text{ave}}}{{L_{2,\text{ave}}}^2}\right) \tag{7}$$

both the de-spin time and system displacement increase by a high power with the separation distance. As such, as close as possible a formation is desirable for the de-spin operations, while successfully mitigating collision risks.

System Scale

Next, consider what happens when the entire system scales up or down in size, while the relative object sizes and separation distance stay constant. This exercise proves useful when considering the downsized terrestrial experiments conducted in Reference 9 and 4, hereby relating the results to the full scale mission design. While the capacitance of each object increases with increasing size, resulting in higher charge levels for a given voltage, the increased separation distance reduces the electrostatic effects. Interestingly, the Coulomb force averaged over one cylinder rotation stays constant with a varying system size scale, while the average arresting torque increases linearly as the system size increases. Assuming that the craft maintain a constant density of 100 kg/m^3 as the sizes scale, the cylinder mass and inertia increase accordingly:

$$m_2 \sim \text{scale}_2{}^3 \tag{8}$$

$$I_2 \sim \text{scale}_2{}^5 \tag{9}$$

Previous work suggests a linear correlation between satellite launch mass and equivalent radius,[12] in which case the mass scales linearly while the inertia scales cubicly. From Eq. (3) and (7), the de-spin time and system displacement increase drastically as the entire system size increases, making it harder to de-tumble large debris satellites even if the control craft increases equally in size. For the same reason, the electrostatic de-spin concept is not feasible for removing the rotation from large asteroid bodies.

Servicing Craft Size

A likely mission scenario is one where the goal is to de-spin a given satellite with specific dimensions. In this case, when designing the mission, the servicing spacecraft must be sized to optimize de-spin performance. The averaged single rotation simulation is run for various servicing craft diameters (where the baseline is a 1 m diameter), while the surface to surface separation distance is held constant at 5 m. Because the MSM spheres used to model the servicing craft spread further and further apart as the craft grows, a higher fidelity model is used with 138 spheres on the debris cylinder and 100 spheres on the control craft. As can be seen in Figure 4, the averaged Coulomb force and torque initially grow with increasing servicing craft diameter, because the capacitance and the charge increase for a given control voltage. At larger diameters, however, the Coulomb torque drops back off because the charge that is distributed along the nonadjacent surface of the control craft becomes further and further removed from the debris cylinder. As a result, the optimal de-spin performance considering this particular cylinder occurs with a control craft diameter of 7.9 m, with diminishing returns evident at larger sizes. The system displacement is minimized at a control craft diameter of 2.6 m. Besides this tradeoff, one must consider the added structural complexity, launch cost, and charging power requirements of flying a large servicing craft.

Debris Aspect Ratio

While not a mission design parameter, it is important to consider what effect the aspect ratio of the debris object has on performance, so that suitable targets for de-spin operations may be selected. Figure 5 shows how the simulation results depend on a varying cylinder length, while the diameter is held constant at 1 m. It is assumed that the same minimum surface to surface separation distance is maintained to mitigate the collision risk. Again, the higher fidelity MSM is used, with the same sphere spacing as above (the number of spheres used on the cylinder now

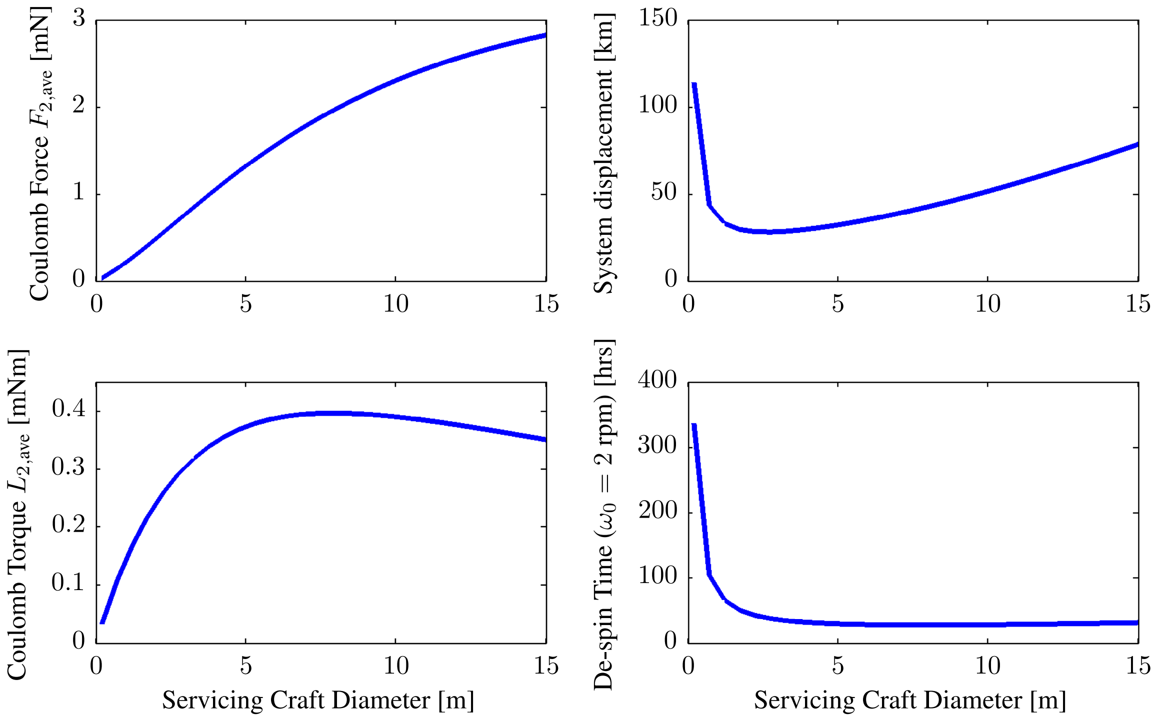

Figure 4. Performance dependency on servicing craft size

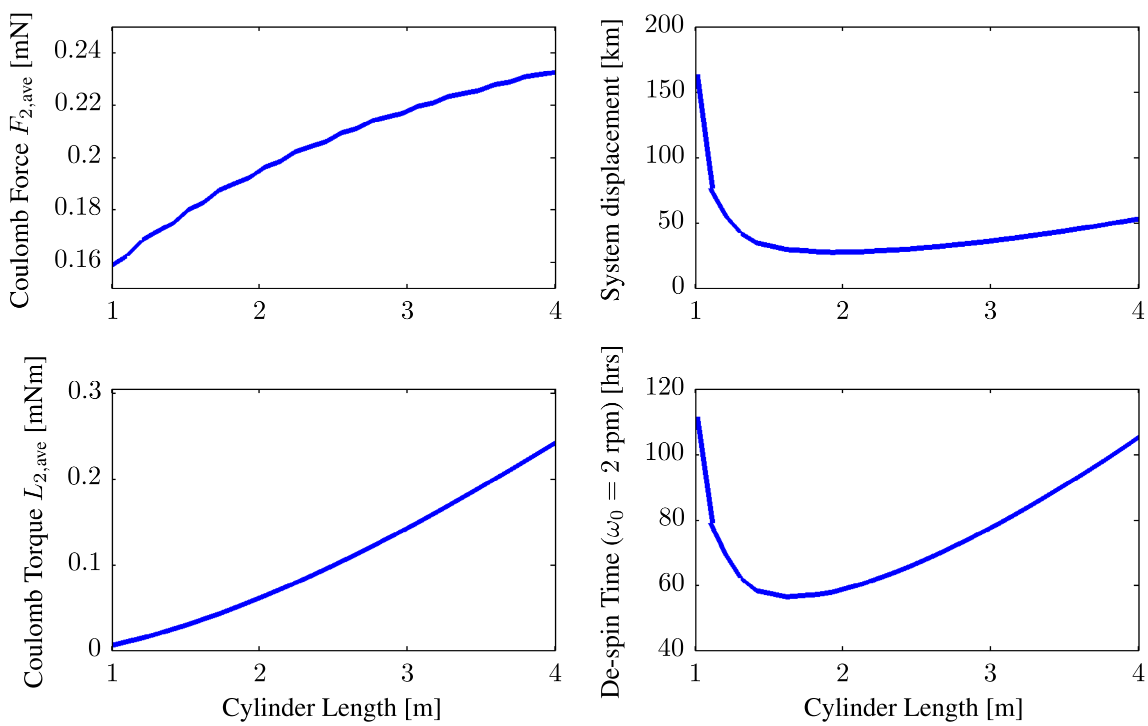

Figure 5. Performance dependency on debris aspect ratio

depends on cylinder length). Interestingly, the shortest de-spin time occurs with a cylinder of length 1.6 m, which represents a relatively small aspect ratio. While a longer aspect ratio results in higher Coulomb torques due to a larger moment arm, this trend is only roughly linear because the center to center separation distance also increases as the cylinder length grows. Mass increases linearly with cylinder length, while the moment of inertia increases to higher order. As a result the de-spin time and system displacement become larger for more slender cylinders.

RELATIVE POSITION AND ORIENTATION CONTROL SCHEMES

Besides designing the remote electrostatic de-spin mission with optimal sizing parameters as deduced from the previous section, the servicing spacecraft has the freedom to control its position and orientation in space with respect to the rotating debris object. The effects of several novel control schemes are herein analyzed. Generally, these approaches result in improvements in de-spin performance, which come at the cost of increased control forces and torques and therefore greater expenditures of fuel or power. The results, as discussed in the following sections, are compared to the baseline simulation and outlined in Table 2.

Table 2. De-spin control schemes results

	Δt [hrs]	ΔX [km]	$F_{\text{thrust,ave}}$ [N]	$L_{\text{att,ave}}$ [Nm]
Baseline	74.32	34.35	0.001296	N.A.
Variable Separation Distance	65.27	31.29	2.073	N.A.
Circumnavigation	37.56	N.A.	5.402	N.A.
Non-spherical Control Craft	56.88	29.62	0.001185	0.09974

Variable Separation Distance

In the baseline control scheme, the center to center separation distance between the two craft is held constant. In order to mitigate the collision risk that poses a threat to mission success, it is actually the surface to surface separation distance that should be maintained at a minimum distance. Therefore, a position control scheme is envisioned where the control craft moves back and forth along the straight line of separation as the cylindrical debris rotates, maintaining a constant separation from the closest surface. Figure 6 shows the resulting desired center to center separation distance of the objects over one full rotation of the cylinder. As is evident, the control craft moves slightly further away than the baseline 7 m separation when the edge of the spinning cylinder is at closest approach.

A proportional-derivative position feedback control is implemented, utilizing the analytic derivative of the desired separation. This control maintains the relative position of the craft to within 0.021 m of the desired separation. Table 2 shows that the time to de-spin 12 deg/s of rotation decreases to 65.27 hours, which represents a 12.1% increase in performance. However, the average required thrusting force increases dramatically to 2.073 N, which falls outside the range of most existing fuel-efficient propulsion technology, and would require several hundred kilograms of expended fuel using conventional bi-propellant thrusters. One can conclude that the marginal gains in performance are not worth such a large cost in fuel requirements.

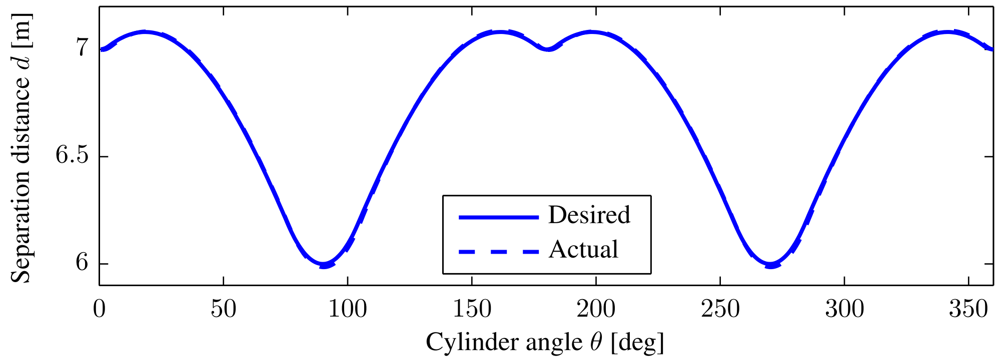

Figure 6. Object separation for constant surface to surface distance

Circumnavigation Scheme

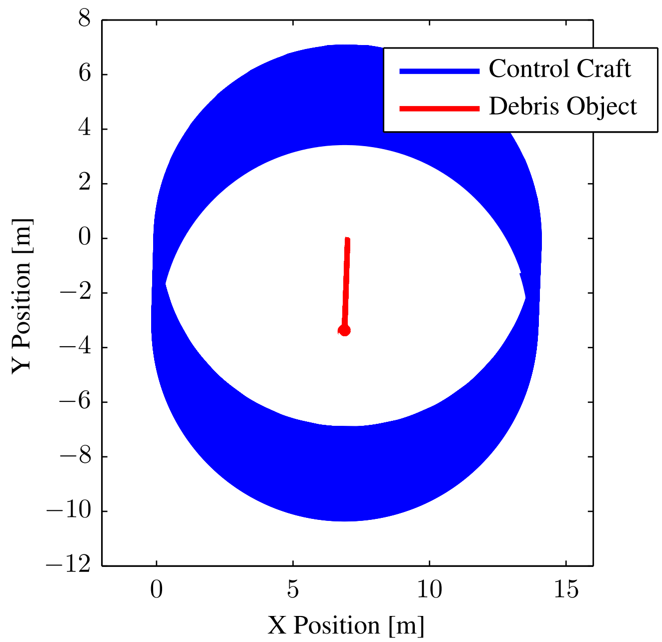

Figure 7. Position of craft in circumnavigation scheme

As the nonspherical debris object rotates, there are certain configurations for which the Coulomb control torque diminishes. Namely, when the cylinder is oriented parallel or perpendicular to the spherical servicer, no electrostatic moment is achievable. This presents the motivation for the following position control scheme, where the servicing craft circumnavigates the debris object as it rotates in order to maintain the optimal relative angle to the cylinder for maximum control torque. The same position control algorithm as before is used with larger gains to maintain a relative angle of $\theta = 42.38°$, at which the cylinder experiences the maximum torque. As can be seen in Figure 7, this scheme results in a very minute system displacement because the net Coulomb forces cancel out as the servicing craft rotates around the debris object. Because the system constantly experiences the maximum achievable torque, de-spin time is reduced by 49.5% to a mere 37.56 hours. As in the previous simulation, the thrusting force necessary to maintain this relative orbit increases several orders of magnitude to 5.402 N. In this scenario, the fuel requirement might be reduced if certain natural circumnavigation formation flying orbits are employed, as will be addressed during future investigations.

Non-spherical Control Craft

Next, a scenario is considered wherein the control craft is no longer modeled as a conducting sphere. If de-spin gains can be achieved by adjusting the attitude of the servicer, it may be possible to improve mission performance by use of rechargeable attitude control devices rather than expending thruster fuel reserves. While a cylindrical control craft was first considered, the desired attitude profile is much more efficient using the windmill configuration depicted in Figure 8. While the dimensions of the three sphere MSM are used, it is assumed that each of the external spheres can be charged independently. A constant relative position $d = 8$ m is maintained between the spacecraft, which represents the same surface to surface separation as before. Now, however, the control craft can adjust its relative orientation to the rotating debris cylinder and specify a voltage $\phi_{1,i} = \pm 30$ kV on any of the four external craft while the rest of the body is held at 0 kV. This will require a complex configuration of charge control devices and charge isolation surfaces.

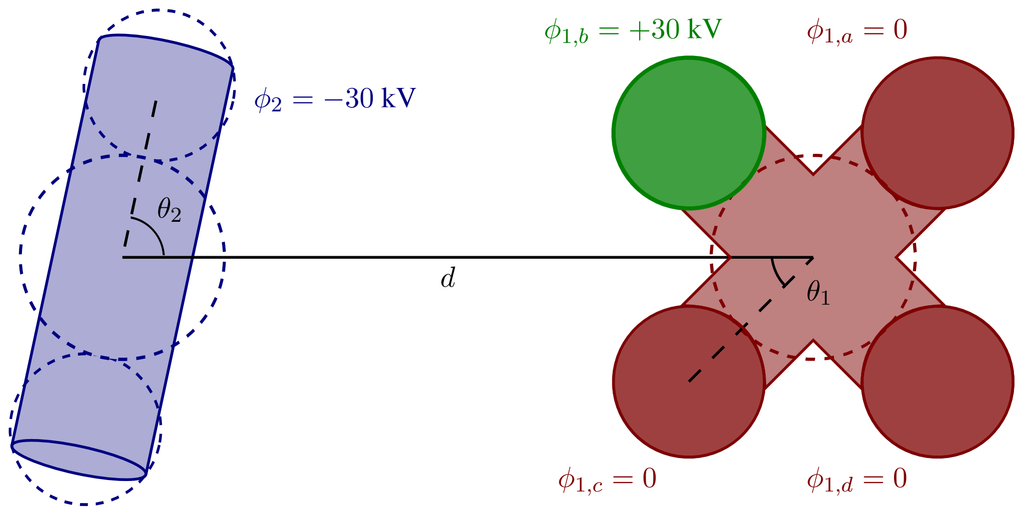

Figure 8. Configuration for windmill control craft

In order to determine an appropriate control strategy, Figure 9 shows the Coulomb torque experienced by the debris cylinder, dependent on the orientation of both objects. The control craft angle θ_1 varies between $-90°$ and $+90°$, which corresponds to one of the two closest spheres in Figure 8 being charged. With the potential of the debris cylinder held at $\phi_2 = -30$ kV, the left plot shows the attractive torques resulting from $\phi_{1,i} = +30$ kV while the right plot shows the lesser torques that result from $\phi_{1,i} = -30$ kV. The superimposed lines show the maximum achievable counter-clockwise (red) and clockwise (blue) torque that is possible for a given debris object orientation θ_2. From this, one can deduce the desired servicing craft attitude θ_1 and which sphere should be charged. If the cylinder in Figure 8 with orientation $\theta_2 \approx 80°$ is spinning counter-clockwise, we wish to arrest it with a clockwise torque. Accordingly, an attractive torque should be applied with $\theta_1 \approx -45°$; thus an electric potential $\phi_{1,b} = +30$ kV must be applied to sphere b.

The results for the first minute of the scenario where the control craft can determine its relative orientation and which component is charged up are displayed in Figure 10. The top plot shows what desired angle is determined from the data in Figure 9, what angle this corresponds to for the craft once the appropriate sphere to charge is chosen, and what angle is achieved by the attitude control algorithm during the simulation. A proportional-derivative control algorithm is implemented, where the desired rotation rate is assumed to be equivalent to the debris rotation (a linearization of the curves in Figure 9). The middle plot in Figure 10 shows which sphere is given what voltage, and the bottom plot shows the required control moments on the servicing craft. In Table 2, it is clear that the time to remove a 12 deg/s rotation on the debris object takes only 56.88 hours, a 23.5% improvement

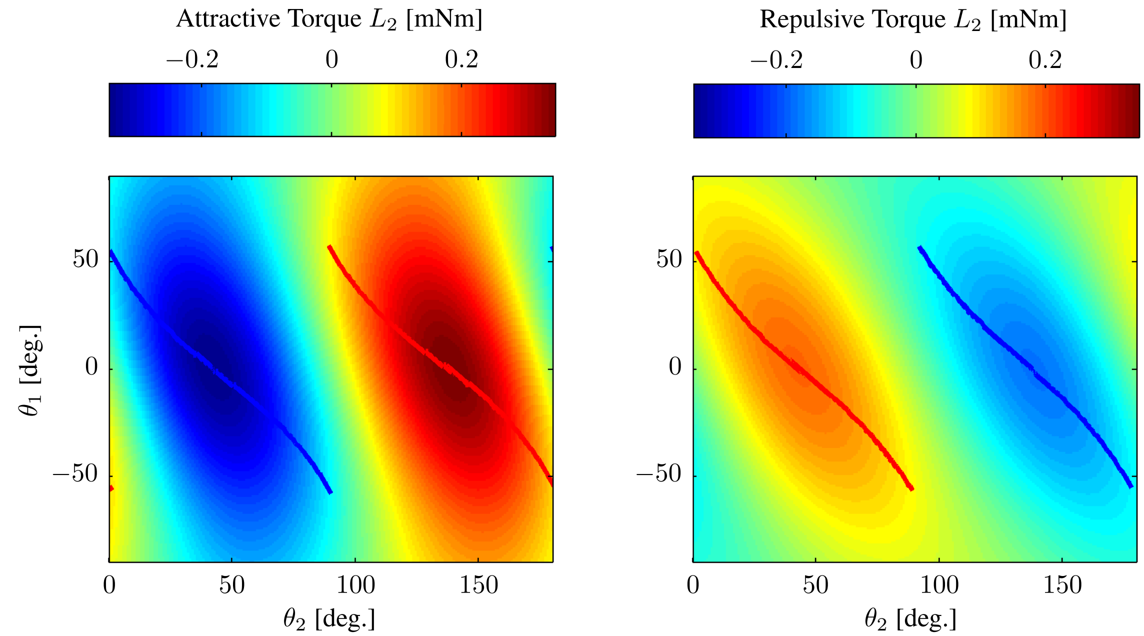

Figure 9. Coulomb torque dependency on debris and control craft angles

in performance. System displacement and required thrusting are reduced, while only an average of less than one tenth of a Nm control moments are required, easily achievable using conventional reaction wheels. Moreover, since the required torques are symmetric, the control moment devices will not require frequent momentum dumping. Therefore, this scenario represents a considerable performance benefit without a significant fuel cost.

CONCLUSION

The optimization study conducted herein is important for future design of mission parameters for the remote electrostatic de-spin concept. In order to perform a proper mission design, sensitivity of the de-spin performance to spacecraft size, shape, and relative position is crucial. Moreover, the desired relative position profiles affect maneuvering and attitude control system requirements. First, it is clear that the closer a servicing spacecraft can get to the rotating debris, the quicker the rotation rate can be reduced, but this objective must be carefully weighed with the collision risks associated with close proximity formation flight. Next, a smaller debris object can be brought to rest quicker, mostly because the moment of inertia and therefore the rotational kinetic energy grow very quickly with size. Because the increased torques are influenced less dramatically by debris aspect ratio, a fairly short cylindrical object is actually optimal for rotation removal. For a given debris target, increasing the size of the servicing craft will increase performance but only up to a given point, which must be balanced with the structural complexities of building large craft. De-spin times can also be reduced if the control craft can be positioned so that it exerts the maximum possible arresting torques on the spinning debris, either by moving closer and further to maintain a constant surface to surface separation, or by circumnavigating the debris to maintain an optimal relative orientation. In both of these scenarios, however, increased amounts of fuel are expended at high thrust levels, thus complicating mission requirements. Lastly, a non-spherical control craft can be designed with multiple voltage controlled features, which are placed in optimal locations by attitude control of

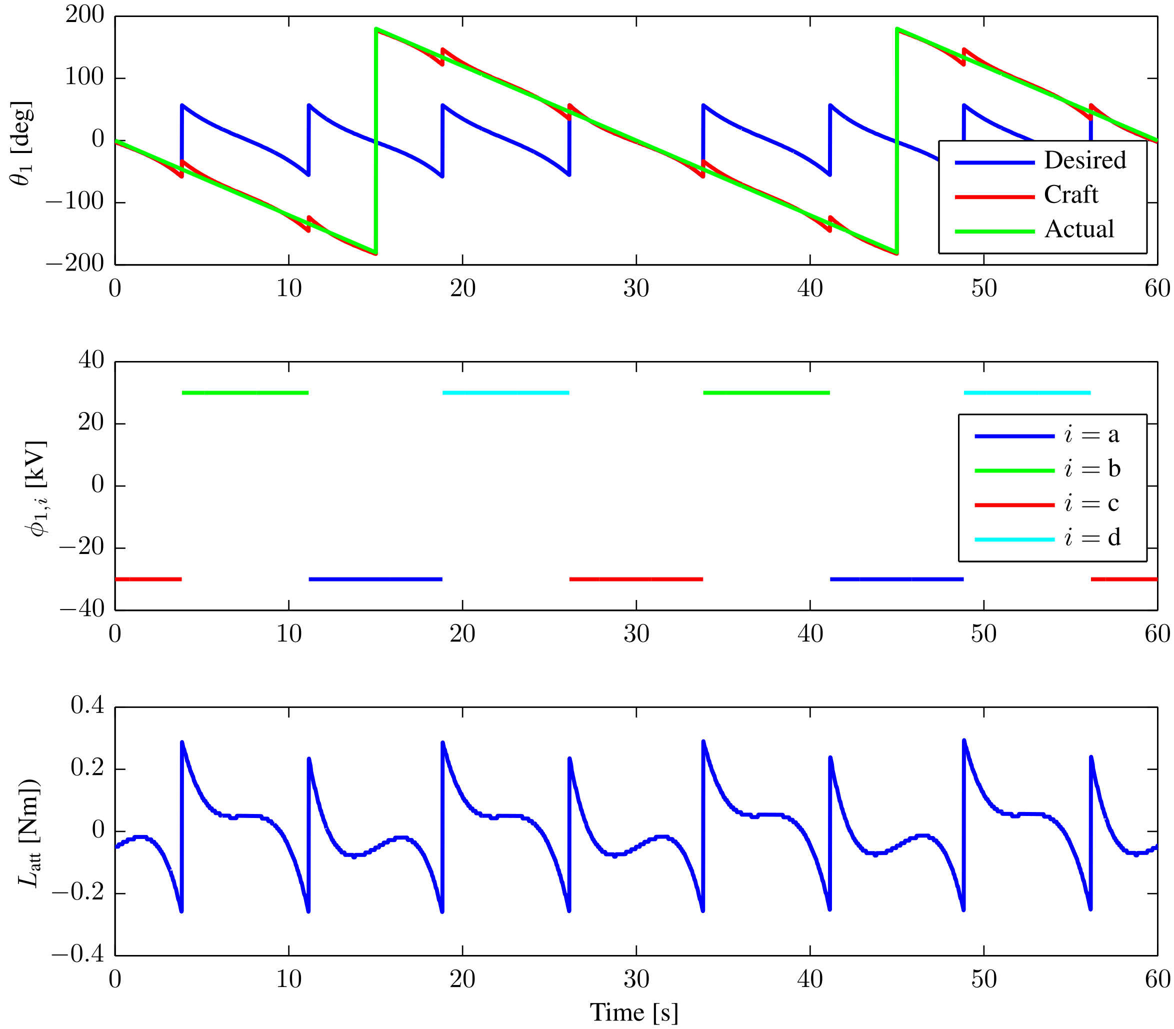

Figure 10. Results from windmill control craft scenario

the craft. With this approach, the debris de-spin time is reduced with only the cost of actuation by rechargeable attitude control devices.

REFERENCES

[1] P. Couzin, F. Teti, and R. Rembala, "Active Removal of Large Debris : Rendez-vous and Robotic Capture Issues," *2nd European Workshop on Active Debris Removal*, Paris, France, 2012. Paper #7.5.

[2] R. Rembala, F. Teti, and P. Couzin, "Operations Concept for the Robotic Capture of Large Orbital Debris," *35th Annual AAS Guidance & Control Conference*, Breckenridge, Colorado, AAS, February 3–8 2012. Paper No. AAS 12-018.

[3] T. Bennett, D. Stevenson, E. Hogan, L. McManus, and H. Schaub, "Prospects and Challenges of Touchless Debris Despinning Using Electrostatics," *3rd European Workshop on Space Debris Modeling and Remediation*, CNES, Paris, June 16–18 2014. Paper #P8.

[4] D. Stevenson and H. Schaub, "Advances In Experimental Verification Of Remote Spacecraft Attitude Control By Coulomb Charging," *GNC 2014: 9th International ESA Conference on Guidance, Navigation and Control Systems*, Porto, Portugal, June 2–6 2014.

[5] H. Schaub and D. Stevenson, "Prospects Of Relative Attitude Control Using Coulomb Actuation," *Jer-Nan Juang Astrodynamics Symposium*, College Station, TX, June 25–26 2012. Paper AAS 12–607.

[6] T. Bennett and H. Schaub, "Touchless Electrostatic Three-Dimensional Detumbling of Large GEO Debris," *AAS/AIAA Spaceflight Mechanics Meeting*, Santa Fe, New Mexico, Jan. 26–30 2014. Paper AAS 14-378.

[7] D. Stevenson and H. Schaub, "Multi-Sphere Method for Modeling Spacecraft Electrostatic Forces and Torques," *Advances in Space Research*, 2012.

[8] D. Stevenson and H. Schaub, "Optimization of Sphere Population for Electrostatic Multi Sphere Model," *IEEE Transactions on Plasma Science*, Vol. 41, Dec. 213, pp. 3526–3535, 10.1109/TPS.2013.2283716.

[9] D. Stevenson and H. Schaub, "Terrestrial Testbed for Remote Coulomb Spacecraft Rotation Control," *International Journal of Space Science and Engineering*, Vol. 2, No. 1, 2014, pp. 96–112.

[10] H. Schaub and Z. Sternovský, "Active Space Debris Charging for Contactless Electrostatic Disposal Maneuvers," *6th European Conference on Space Debris*, Darmstadt, Germany, ESOC, April 22–25 2013. Paper No. 6b.O-5.

[11] E. A. Hogan and H. Schaub, "Impacts of Tug and Debris Sizes on Electrostatic Tractor Charging Performance," *International High Power Laser Ablation and Beamed Energy Propulsion*, Santa Fe, New Mexico, April 21–25 2014.

[12] H. Schaub and L. E. Z. Jasper, "Orbit Boosting Maneuvers for Two-Craft Coulomb Formations," *AIAA Journal of Guidance, Control, and Dynamics*, Vol. 36, Jan. – Feb. 2013, pp. 74–82, 10.2514/1.57479.